IOP Conf. Series: Materials Science and Engineering **276** (2017) 012022 doi:10.1088/1757-899X/276/1/012022

Finite element simulation of long wave impact on floating breakwaters with variable stiffness

T K Papathanasiou[1]*, **A Karperaki**[2] **and K A Belibassakis**[3]

[1]Department of Mechanical, Aerospace and Civil Engineering, Brunel University London, Uxbridge UB8 3PH, UK
[2]School of Naval Architecture and Marine Engineering, National Technical University of Athens, Zografos, 15773, Greece
[3]School of Naval Architecture and Marine Engineering, National Technical University of Athens, Zografos, 15773, Greece

*Contact author: theodosios.papathanasiou@brunel.ac.uk

Abstract. The hydroelastic response of flexible, floating breakwaters is a subject of interest for coastal engineering applications. In this study, a higher order hydroelastic finite element is applied to the simulation of floating breakwaters of variable stiffness undergoing long wave impact. The main aim is the evaluation of breakwater efficiency in terms of transmitted and reflected wave characteristics. It is established that, for the wave-lengths examined, the maximum amplitude and wave-length of the transmitted pulse are strongly dependent on the breakwater stiffness. Finally it is shown that for case of a periodic stiffness profile the transmitted energy is minimised when the modulation wavelength is comparable to the wavelength of the incoming excitation.

1. Introduction

Slender flexible floating bodies have been studied by several authors using both analytical [1] and numerical techniques [2]. In the literature, the response of geophysical formations such as ice floes [2-3] and even specific types of floating breakwaters are modelled under thin plate theory assumptions [4-5]. Kirchhoff's classical plate theory becomes relevant as the horizontal dimensions of the structure in question are significantly larger than its thickness, rendering the hydroelastic responses of the floating structure dominant over rigid body motions. A structure complying with the aforementioned assumption of negligible thickness compared to horizontal dimensions is expected to flex under wave excitation, leaving only fractions of the incident wave energy to be transmitted. In turn part of the remaining energy will either reflect or dissipate due to friction and damping [6]. A floating breakwater structure is expected to shelter marinas and harbours in an environment of limited fetch [4-5]. The principal aim of floating breakwater configurations is to mitigate the transmitted wave energy and the transmitted wave amplitude. The investigation of reflection and transmission characteristics of a coupled hydroelastic system yields valuable information for the optimal design of a floating breakwater structure, aiming in wave action attenuation.

Commonly, the linear water wave theory is employed for the study of regular wave reflection and transmission characteristics of a structure resting on a layer of inviscid and irrotational fluid. In this

line of thought, notable are the works of Meylan and Squire [7] and Montiel [8] who study reflection-transmission characteristics for the case of a thin ice floe, with the latter work accounting for the Archimedean draft. In the given investigations the transmission coefficient of the energy conserving system was correlated with the incident wavelength. Bennets et al. [9] and Smith and Meylan [10] explored the effects of plate thickness in the computed transmitted energy.

As already mentioned the Kirchoff thin plate assumptions are employed for structures with small thickness-to-length ratio. Moreover, as floating breakwaters are positioned near-shore the study in a shallow depth environment is relevant. In that note, Sturova [11] studied the transient response of a thin, heterogeneous plate in shallow water conditions by means of an eigenfunction expansion method. Additionally, Praveen et al [12] considered in their work, the hydroelastic response of a thick plate under the long wave assumptions. However, in nearshore environments the abrupt variability of the bathymetry must also be taken into account. Papathanasiou et al. [13] presented a higher order finite element scheme for the solution of the transient hydroelastic problem featuring a thin, heterogeneous plate, floating over variable, shallow bathymetry.

In the present contribution, we focus on the determination of reflection-transmission coefficients for the coupled hydroelastic system involving a thin, elastic strip featuring inhomogeneities, which interacts with incoming long waves. The motivation of the present study lays in the analysis and design of novel breakwater configurations. In addition, the present investigation is able to provide a simple tool for determining regions of excessive wave energy transmission for harvesting purposes. A similar study was conducted by the authors in [14] focusing on the effects of bathymetry on the reflected and transmitted wave characteristics. In this contribution we focus on the effect of the elastic modulus of the floating structure. A parametric study, involving several modulation types of the stiffness value along the breakwater is performed and optimal stiffness variations are determined. The optimization criteria involve the minimization of energy and maximum wave amplitude in the transmission region. Locally increased breakwater stiffness properties can also be achieved through the use of elastic connections to the seabed [15]. The response of flexible breakwaters, elastically connected to the seabed is studied in the same framework too. These, very local in nature, stiffness enhancements are found to induce significant alterations in the wave reflection properties of the breakwaters.

2. Organization of paper

The present paper is structured as follows: Section III briefly presents the governing mathematical equations for the problem of calculating the flexural, hydroelastic response of a floating, thin plate over shallow water bathymetry. Section IV explores the variational form of the presented initial boundary value problem and presents the implementation of the proposed finite element scheme. Section V presents a series of numerical results exploring the reflected and transmitted wave characteristics, firstly for the case of a breakwater with constant stiffness and then for the case of a breakwater featuring variable Young's modulus. Finally, in Section VI key findings are summarized and further research is proposed.

3. Governing equations

In the present section, the governing equations for a coupled hydroelastic problem featuring a thin, floating plate over shallow waters will be briefly presented. The reader is directed to relevant works in the literature for a more in depth discussion [2,11,13]. A two dimensional Cartesian coordinate system is employed, with the horizontal axis x coordinate system coinciding with the mean water level, and the vertical axis z pointed upwards. The plate is assumed to extend indefinitely in the direction vertical to the xz plane. The case of a flexible elastic strip is therefore considered. The respective 1D domain $\Omega:(-\infty < x < \infty)$ is occupied by a layer of inviscid and irrotational fluid. The floating elastic strip is located at the 1D domain extending from $x=0$ to $x=L$. The thickness distribution of the flexible strip is $\tau(x)$ and its density ρ_p. The density of the fluid (water) is denote by ρ_w.

The symbols S_0, S_1, S_2 will be used to denote the three subregions $0 < x < L$, $-\infty < x < 0$ and $L < 0 < +\infty$, respectively (see also Figure 1). The three regions will be termed 'region of hydroelastic interaction', 'region of transmission' and 'region of reflection' respectively. In S_0 the free water surface elevation $\eta(x,t)$ is assumed to coincide with the plate deflection. The velocity potential functions $\varphi_i, i = 0,1,2$ will be used for the three abovementioned domains. The bathymetry in the domain of 'hydroelastic interaction' is given by $s(x) - d(x)$, where $s(x)$ is the variable depth of the seabed with respect to the undisturbed free surface and $d(x) = \rho_p \rho_w^{-1} \tau(x)$ is the plate draft (according to Archimedes principle). The semi-infinite, thin strip assumption allows for the modelling of the plate by means of the Euler-Bernoulli beam theory. For the hydrodynamic modeling, the linearized Shallow Water Equations are employed. The following non-dimensional variables are employed for the derivation of the resulting 1-D hydroelastic system,
$\tilde{x} = x / L$, $\tilde{\eta} = \eta / L$, $\tilde{t} = g^{1/2} L^{-1/2} t$ and $\tilde{\varphi}_i = g^{-1/2} L^{-3/2} \varphi_i$, for $i = 0,1,2$

After dropping tildes for simplicity the non-dimensional system is written as,

$$M\ddot{\eta} + \left(K\eta_{xx}\right)_{xx} + \eta + \dot{\varphi}_0 = 0, \; x \in S_0, \tag{1}$$

$$\dot{\eta} + (H\varphi_{0x})_x = 0, \; x \in S_0, \tag{2}$$

$$\ddot{\varphi}_1 - (H\varphi_{1x})_x = 0, \; x \in S_1, \tag{3}$$

$$\ddot{\varphi}_2 - (H\varphi_{2x})_x = 0, \; x \in S_2, \tag{4}$$

with the coefficients $M(x) = m(x)\rho_w^{-1} L^{-1}$, $K = D\rho_w^{-1} g^{-1} L^{-4}$, $H(x) = \left[s(x) - d(x)\right] / L$ in the 'hydroelastic interaction' region, $H(x) = s(x) / L$ outside the 'hydroelastic interaction' region and g the acceleration of gravity. The flexural rigidity of the plate is $D = E\tau^3 (12(1-\nu^2))^{-1}$, where E is the Young's modulus and ν the Poisson's ratio of the plate material. The non-dimensionalised quiescence conditions at infinity are given as

$$\varphi_{1x} = 0 (x \to -\infty) \text{ and } \varphi_{2x} = 0 (x \to \infty). \tag{5}$$

At the interfaces between subregions, mass and energy conservation dictated the following matching conditions

$$H(0^-)\varphi_{1x}(0^-,t) = H(0^+)\varphi_{0x}(0^+,t), \tag{6a}$$

$$H(1^-)\varphi_{0x}(1^-,t) = H(1^+)\varphi_{2x}(1^+,t), \tag{6b}$$

$$\dot{\varphi}_1(1^-,t) = \dot{\varphi}_0(1^+,t) \text{ and } \dot{\varphi}_0(1^-,t) = \dot{\varphi}_2(1^+,t). \tag{7}$$

For a freely floating plate, the non-dimensional boundary conditions at the edges, corresponding to zero shear force and bending moment, are

$$K\eta_{xx}\big|_{x=0} = 0, \; K\eta_{xx}\big|_{x=1} = 0 \text{ and} \tag{8}$$

$$K\eta_{xxx}\big|_{x=0} = 0, \quad K\eta_{xxx}\big|_{x=1} = 0. \tag{9}$$

The initial- boundary value problem is completed with appropriate initial conditions of the form

$$\eta_0(x,0) = \phi_0(x,0) = 0, \; x \in S_0, \tag{10}$$

$$\phi_1(x,0) = \partial_t \phi_1(x,0) = 0, \tag{11}$$

$$\phi_2(x,0) = 0, \; \partial_t \phi_2(x,0) = -G(x), \tag{12}$$

The above initial conditions imply that an initial upper surface disturbance, denoted by $G(x)$, is allowed to propagate at the offshore region S_2 at the beginning of time, while the free water surface in region S_1 and the upper surface in the hydroelastic coupling region S_0 are at rest.

4. Finite element implementation

The weak form of the above initial-boundary value problem is subsequently derived by the employment of appropriate weight functions. The procedure is described in detail in [13] and briefly outlined below for completeness in presentation. The presented Equations (1)-(4), valid in given subregions of $\Omega:(-\infty<x<\infty)$, are multiplied with the corresponding weight functions: $v\in H^2(S_0)$, $-w_0\in H^1(S_0)$, $w_1\in H^1(S_1)$, $w_2\in H^1(S_2)$, where H^k is the space of functions with square integrable *k* order derivative, and finally integrated over the respective subdomains . After performing integration by parts,

$$\int_0^1 Mv\ddot{\eta}dx+\int_0^1 Kv_{xx}\eta_{xx}dx+\int_0^1 v\eta dx+\int_0^1 v\dot{\varphi}_0dx=0 \tag{13}$$

$$-\int_0^1 w_0\dot{\eta}dx+\int_0^1 w_{0x}H\varphi_{0x}dx-\left[w_0H\varphi_{0x}\right]_0^1=0 \tag{14}$$

$$\int_{-\infty}^0 w_1\ddot{\varphi}_1dx+\int_{-\infty}^0 w_{1x}H\varphi_{1x}dx-\left[w_1H\varphi_{1x}\right]_{-\infty}^0=0 \tag{15}$$

$$\int_1^\infty w_2\ddot{\varphi}_2dx+\int_1^\infty w_{2x}H\varphi_{2x}dx-\left[w_2H\varphi_{2x}\right]_1^\infty=0 \tag{16}$$

Adding Equations (13)-(16) and the employment of the quiescent conditions at infinity and the matching conditions imposed by material continuity at the interfaces results in the formulation of the following variational problem,

Find $\eta(x,t)$, $\varphi_0(x,t)$ $\varphi_1(x,t)$ and $\varphi_2(x,t)$ such that for all $v\in H^2(S_0)$, $-w_0\in H^1(S_0)$, $w_1\in H^1(S_1)$ and $w_2\in H^1(S_2)$ it is

$$\begin{aligned}&\int_0^1 Mv\ddot{\eta}dx-\int_0^1 w_0\dot{\eta}dx+\int_{-\infty}^0 w_1\ddot{\varphi}_1dx+\int_1^\infty w_2\ddot{\varphi}_2dx\\&\quad+a(\eta,v)+b_0(\varphi_0,w_0)+b_1(\varphi_1,w_1)+b_2(\varphi_2,w_2)=0\end{aligned} \tag{17}$$

where the bilinear functionals appearing in (17), are defined as:

$a(\eta,v)=\int_0^1\left(Kv_{xx}\eta_{xx}+v\eta\right)dx$, $b_0(\varphi_0,w_0)=\int_0^1 w_{0x}H\varphi_{0x}dx$, $b_1(\varphi_1,w_1)=\int_{-\infty}^0 w_{1x}H\varphi_{1x}dx$ and $b_2(\varphi_2,w_2)=\int_1^\infty w_{2x}H\varphi_{2x}dx$.

In Papathanasiou et al. [13], it is shown that for the examined hydroelastic system the following quantity, which is actually the energy of the system, is conserved,

$$\begin{aligned}\mathcal{E}(t)=&\left(\int_0^1 M\dot{\eta}^2dx\right)+\left(\int_{-\infty}^0\dot{\varphi}_1^{\,2}dx\right)+\left(\int_1^\infty\dot{\varphi}_2^{\,2}dx\right)+a(\eta,\eta)\\&+b_0(\varphi_0,\varphi_0)+b_1(\varphi_1,\varphi_1)+b_2(\varphi_2,\varphi_2)\end{aligned}. \tag{18}$$

The total energy of the system is proven to be conserved in time and equal to the energy provided form the initial free water surface disturbance, hence it holds that $\mathcal{E}(t)=\mathcal{E}(0)$ for every $0\le t\le T$, where T is the examined time interval.

The above variational problem will be solved by means of the higher order finite element scheme developed in [13]. In particular, we are interested for the solution of the initial boundary value problem corresponding to a long wave pulse generated in the 'transmission region', propagating and interacting with the floating plate. The computational spatial domain that will be used is set such that x extends from $-x_A$ to x_B, where these values define a spatial domain large enough so that the pulses do not reach the computational domain boundaries in the examined time interval. Thus the conditions for the

velocity potential spatial derivative (velocity) at infinity are also valid at the edges of the computational domain.

In the free surface regions, i.e. the 'transmission' and the 'reflection' regions, the velocity potential function is approximated by fourth order Lagrange polynomial shape functions. In the region of hydroelastic coupling a special hydroelastic element introduced in [13] is used. The special element features quantic Herminte polynomials for the approximation of the plate deflection and fourth order Lagrange polynomials for the velocity potential function in the region. Hence, the approximate solution in each element is given as,

$$\eta^h = \sum_{i=1}^{6} H_i(x)\eta_i^h(t) \text{ and } \varphi_j^h = \sum_{i=1}^{5} L_i(x)\varphi_{ij}^h(t),\ j=1,2 \tag{19}$$

Substituting the above expressions in the variational problem defined by Eq. (17) results in a second order system of the form $\mathbf{M}\partial_{tt}u + \mathbf{C}\partial_t u + \mathbf{K}u = 0$, where the vector u contains the nodal unknowns. The implication in this otherwise standard dynamical system is that each matrix is singular. The stability results in [13] however guarantee a unique solution of this discrete system. That is, an appropriate linear combination of the matrices appearing in this dynamic system must be invertible. This fact enforces the application of an implicit time integration procedure. Subsequently, a Newmark time integration scheme (see [13]) is employed in order to calculate the solution of the ordinary differential equation system. The particular values for the Newmark method $\gamma = 1/2$ and $\beta = 1/4$ have been used in all the numerical results that follow. The number of time steps employed is in all cases sufficient to ensure high accuracy.

5. Numerical results

In this section, the efficiency of flexible breakwaters, in terms of reflection and transmission characteristics, will be analysed with respect to the stiffness of the flexible elastic component. More specifically, several types of stiffness distribution along the flexible elastic strip will be considered and the portion of energy transmitted to the near-shore region will be derived. In addition, the distorted form of the main pulse, after interaction with the breakwater, will be calculated and the reduction in amplitude of the transmitted pulse will be studied. Throughout the following analysis the length of breakwater is taken as $L = 250$ m and its thickness is set to $\tau(x) = 0.5$ m. The density of the elastic material of the breakwater is $\rho_p = 900$ kg/m^3 while the water density is $\rho_w = 1025$ kg/m^3. All the numerical results involve an incoming wave created by an initial water surface elevation at the offshore region. This initial upper surface elevation has the general form

$$G(x) = 2A_0 \exp\left(-\mu\left(x - x_0\right)^2\right) \tag{20}$$

where the non-dimensional pulse amplitude is $A_0 = 3.3\cdot 10^{-4}$, while the non-dimensional, positive parameter controlling the smoothness of the pulse is set to $\mu = 250$. Finally, x_0 denoted the point of origin for the initial disturbance located in region S_2. The initial profile splits into a left and a right propagating wave. The right propagating wave travels to the offshore region and is just plotted as a reference wave profile. It is the left propagating wave that interacts with the floating breakwater. Due to the large wavelength of the pulses, compared with the depth of the basin considered, and the related assumption of shallow water hydrodynamics, the pulses remain unaltered when propagating in constant bathymetry regions.

At the hydroelastic region, the bathymetry varies creating a shoal approximated by the function,

$$H\left(x\right) = 4 + 2\tanh\left(10x\right). \tag{21}$$

At this point it is noted that for presentation purposes, and with no loss in the generality of the presented theoretical analysis, the origin of Cartesian axis is horizontally translated so as to include the entire computational domain in the right half-plane. In that line of thought, the employed bathymetry

(21) corresponds to a smooth shoaling profile given by a hyperbolic tangent with the point of inflection coinciding with the middle of the floating breakwater, as seen in Figure 1. In the same figure the initial disturbance is seen to split into two identical pulses with half the initial amplitude travelling is opposite directions and featuring no signs of dispersion as previously mentioned.

5.1. Constant stiffness

At a first step, the case of constant stiffness will be examined. For that, three different examples with breakwaters of constant stiffness will be presented. The first examined case concerns a very flexible floating strip. In particular, the Young's modulus value $E = 5 \cdot 10^7 \ N/m^2$ is considered. Note that the Young's modulus values selected do not represent any specific material but rather the macroscopic elastic behaviour of the floating component. The second constant stiffness case involves a flexible breakwater of intermediate stiffness. The value of Young's modulus selected for this second case is $E = 5 \cdot 10^9 \ N/m^2$. Finally, a very stiff breakwater is introduced and assigned the value $E = 5 \cdot 10^{11} \ N/m^2$.

In Figure 2 snapshots of the propagating pulse impacting the floating breakwater and subsequently transmitting in region S_1 are shown for the case featuring a 'soft' breakwater. The upper surface elevation at the same time instants are depicted in Figure 3 and 4 for the intermediate stiffness and the 'stiff' breakwater cases respectively.

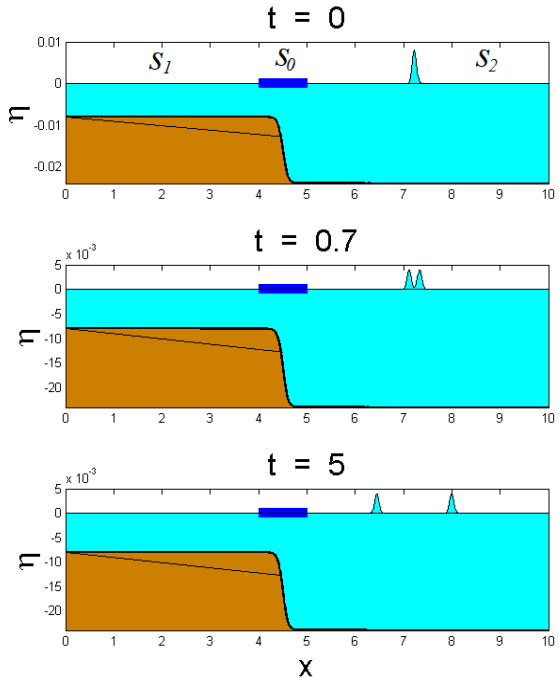

Figure 1. Initial Surface elevation and long wave propagation in the offshore region

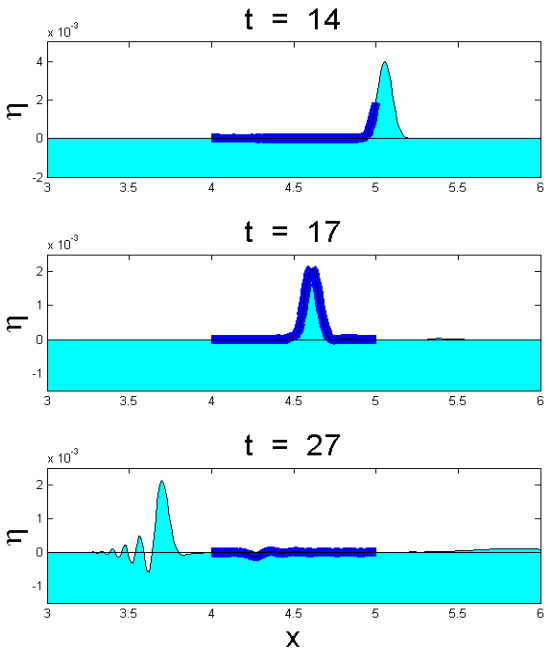

Figure 2. Hydroelastic interaction and transmitted wave profile in the case of a 'soft' flexible breakwater with $E = 5 \cdot 10^7 \ N/m^2$.

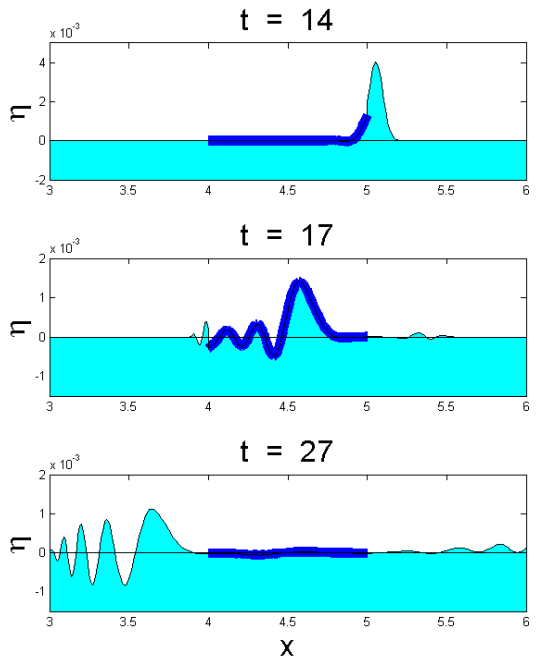

Figure 3. Hydroelastic interaction and transmitted wave profile in the case of a relatively 'stiff' flexible breakwater with $E = 5 \cdot 10^9\ N/m^2$.

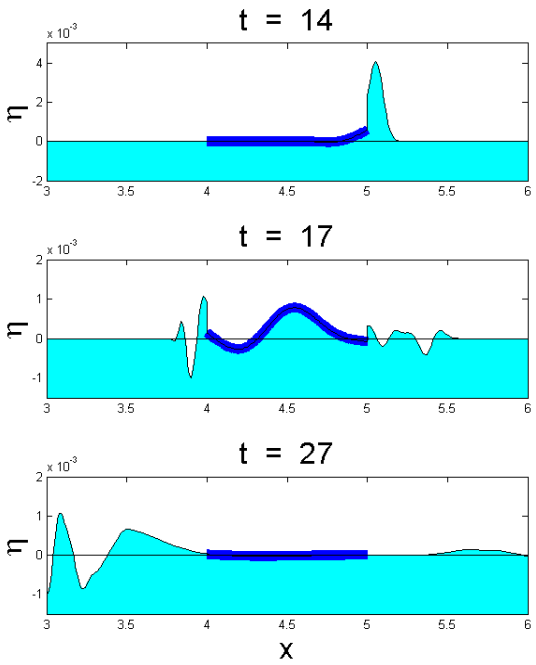

Figure 4. Hydroelastic interaction and transmitted wave profile in the case of a very 'stiff' breakwater with $E = 5 \cdot 10^{11}\ N/m^2$.

Comparing Figures 2, 3, 4 it is readily deduced that as stiffness increases, the amplitude of the reflected pulse is seen to increase while the transmitted wave amplitude is successfully attenuated. Additionally, the 'softer' case in Figure 2 leads to a transmitted pulse with wavelength similar to the initial disturbance that impacts the structure, along with a small dispersive trail. In Figures 3 and 4 however the transmitted pulse appears significantly altered. In Figures 5, 6 and 7 the energy of the system, defined in (18) is illustrated for all the considered constant stiffness cases. The nondimensional total energy of the system $\mathcal{E}$, denoted by the thick black line, is found to be constant in time.

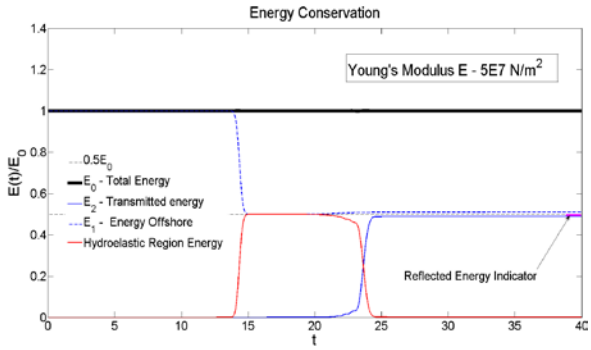

Figure 5. Energy of the system before, during and after the Hydroelastic interaction and portion of the reflected pulse energy in the case of a 'soft' flexible breakwater with $E = 5 \cdot 10^7\ N/m^2$.

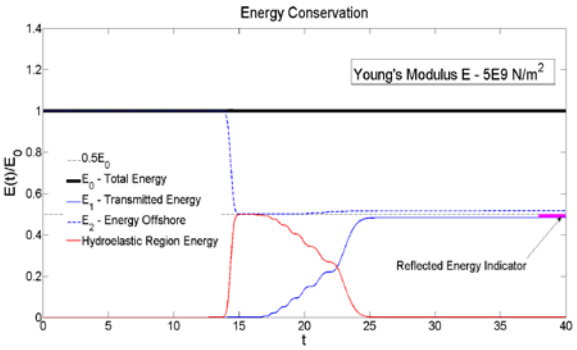

Figure 6. Energy of the system before, during and after the Hydroelastic interaction and portion of the reflected pulse energy in the case of a relatively 'stiff' flexible breakwater with $E = 5 \cdot 10^9\ N/m^2$.

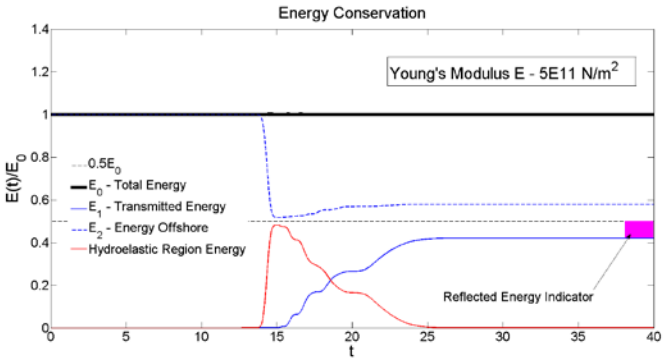

Figure 7. Energy of the system before, during and after the Hydroelastic interaction and portion of the reflected pulse energy in the case of a very 'stiff' breakwater with $E = 5 \cdot 10^{11}\ N/m^2$.

The total energy of the system includes the energy of the pulse that propagates in the offshore region, away from the breakwater. Hence the energy that reaches the structure is half the initial energy of the system. The pulse propagating towards the nearshore region is partly reflected back in S_2 due to the presence of the elastic body and partly transformed into hydroelastic energy before finally being transmitted into S_1. This implies that the energy of the pulse interacting with the breakwater is $0.5\mathcal{E}$. This energy level is depicted in the figures by a thin, dashed line. The energy against time in every subregion is also depicted in the figures. The difference between the transmitted energy in region S_2, given by the continuous blue line and half of the energy that impacts the breakwater is an indicator of the pulse energy that is reflected back in the offshore region. It is clearly seen that the reflected energy increases with increasing elastic stiffness. The given outcome is of interest since maximization of reflection corresponds to the optimal attenuation of transmitted energy.

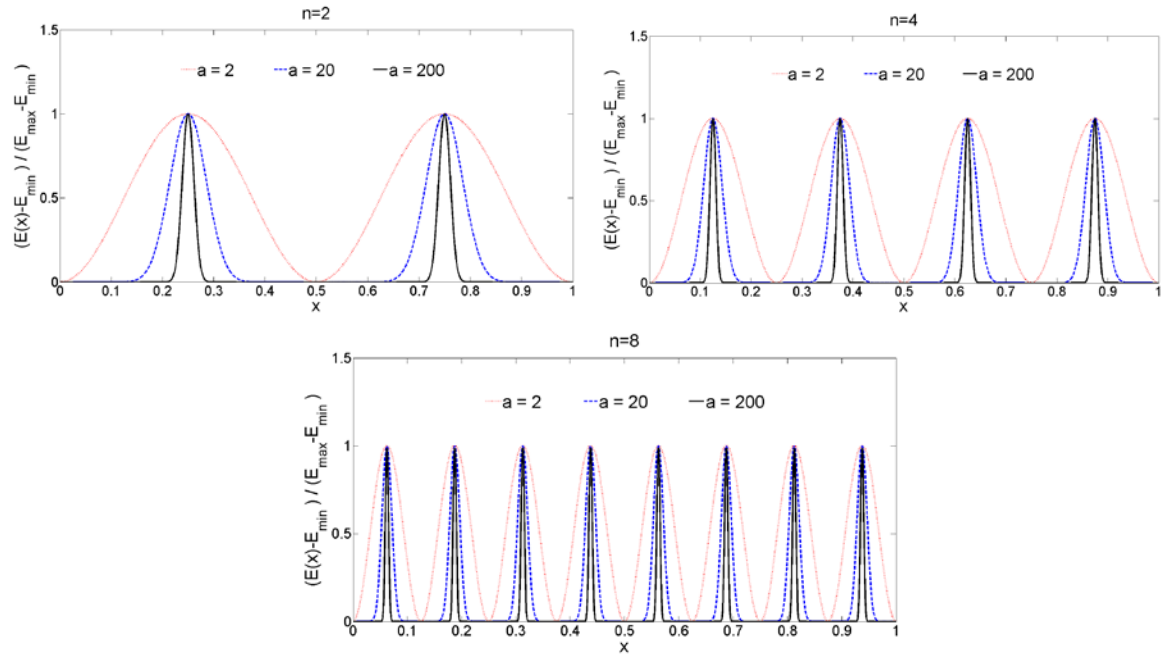

Figure 8. Variation of the elastic modulus along the span of the flexible strip for different values of n and a.

5.2. Variable stiffness

For the analysis of flexible breakwaters with variable stiffness, the following profile for Young's modulus will be adopted

$$E(x) = E_{\min} + \left(E_{\max} - E_{\min}\right)\sin^{a}\left(n\pi(x - x_0)\right). \tag{22}$$

The above distribution suggests that Young's modulus is allowed to vary between a minimum and a maximum value. Parameters a and n that appear in expression (22) affect the shape of the stiffness profile in terms of periodic variation frequency and stiffness of the peaks, as shown in Figure 8. The minimum value of the Young's modulus selected is $E = 5 \cdot 10^{9}\ N/m^2$ while the maximum value selected is $E = 5 \cdot 10^{11}\ N/m^2$. It is evident that significantly increasing the exponent a results in a localized elastic stiffening which is equivalent to the presence of an elastic connection of the breakwater with the seabed at n locations.

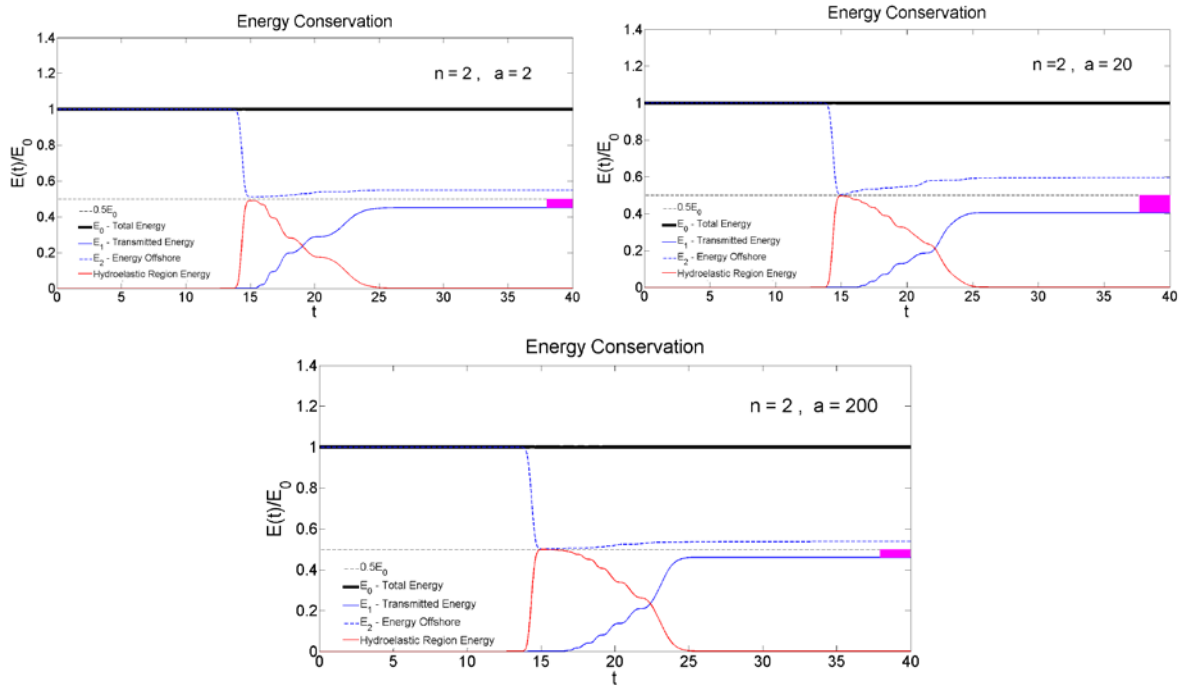

Figure 9. Energy balance and transmitted energy indicator for $n = 2$ and different values of the exponent a.

The reader is referred to the work of Karperaki et al. [15] for an in depth analysis of the hydroelastic response of a thin floating structure, elastically connected to the seabed. The energy balance principle is again explored for several variable stiffness profiles featuring different values of parameters a and n. In Figure 9 the case of a constant number of peaks $n = 2$ in the periodic fluctuation of the Young's modulus is employed. An increasing steepness parameter a is considered. It is seen that the reflected pulse is maximized for the intermediate case of $a = 20$. It is clearly seen however in Figures 9, 10, 11 that the optimum transmitted energy attenuation is achieved for a steepness parameter that depends on the number of peaks in the periodic variation for profile (22). This suggests an optimization problem. More specifically, in Figure 10, where $n = 4$, the maximization of reflected energy is achieved for $a = 2$. For an increased number of periodic fluctuations, as seen in Figure 11, the optimal case is achieved for $a = 20$.

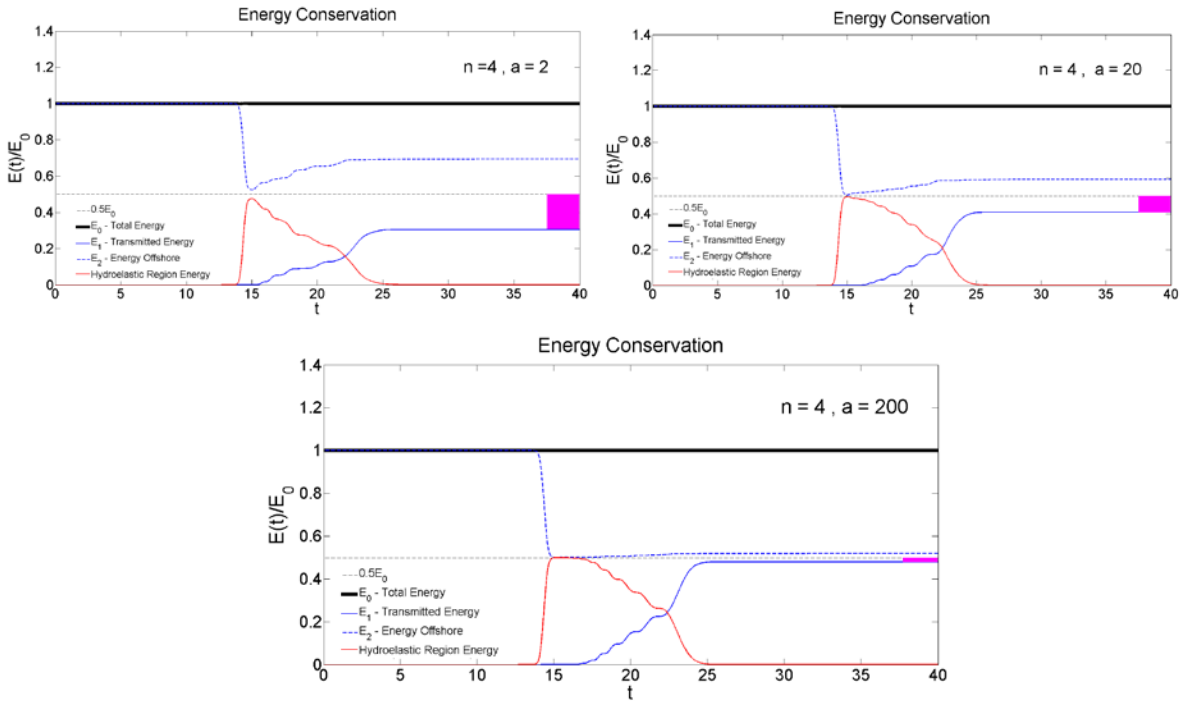

Figure 10. Energy balance and transmitted energy indicator for $n = 4$ and different values of the exponent a.

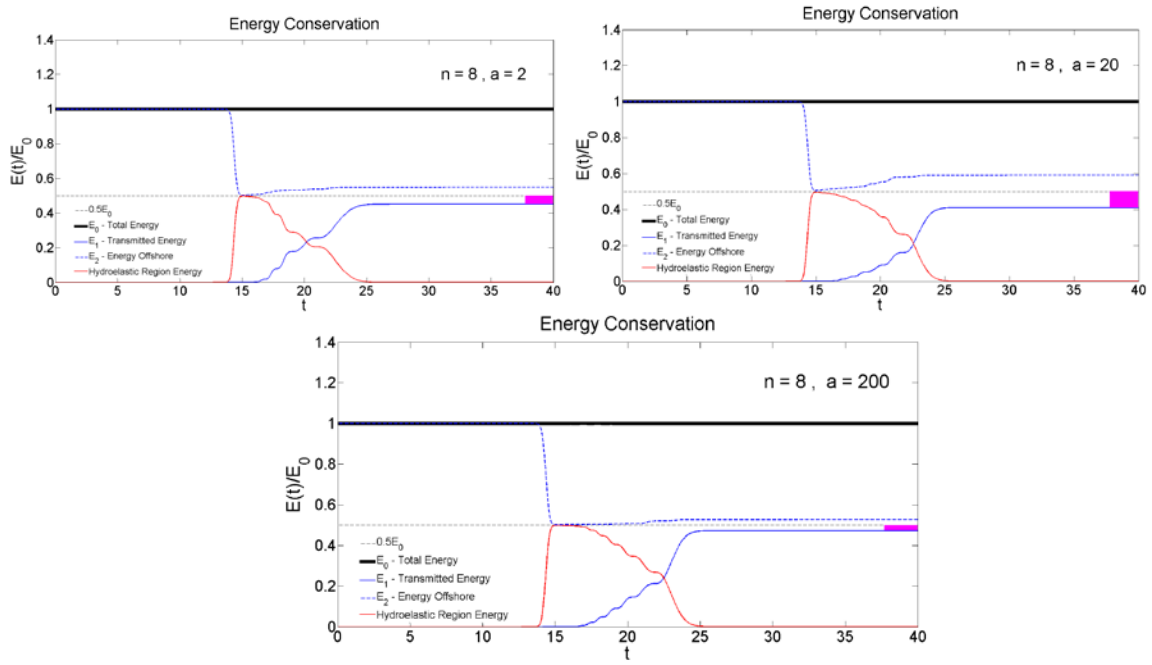

Figure 11. Energy balance and transmitted energy indicator for $n = 8$ and different values of the exponent a.

The given result is fundamentally different from the previous observations for a constant stiffness profile, where increasing the Young's modulus results in decreasing transmitted energy. For the examined stiffness profile, maximization of the reflected energy is achieved when the wavelength of the periodic Young's modulus distribution is comparable with the incoming pulse wavelength. In such cases the hydroelastic pulse suffers multiple reflections that increase the total reflected energy. When

the periodicity of the Young's modulus assumes a wavelength that is much larger than the one of the excitation pulse, the reflected wave energy reduces again.

In order to further investigate the correlation between the parameters a and n a parametric study was conducted for a constant steepness parameter $a=2$ and a varying number of fluctuations. The results of the study shown in Figure 12 suggest that the minimization of the transmitted energy is deduced for $n=5$. In Figure 13, snapshots of the upper surface deflection for the above optimal scenario are shown. The amplitude of the transmitted wave appears significantly reduced when compared to the amplitude of the incoming pulse suggested by the amplitude of the hydroelastic response in $t=15$, just moments after impact.

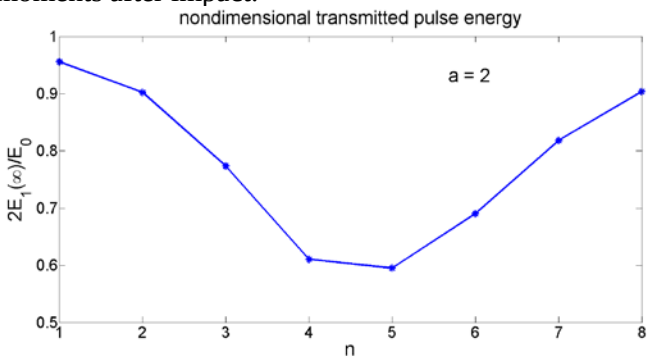

Figure 12. Energy transmitted in the nearshore region for $a=2$ and different values n.

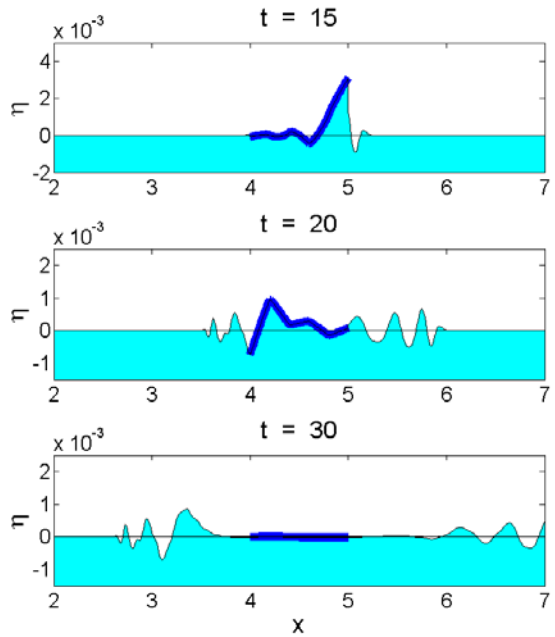

Figure 13. Snapshots of the upper surface elevation for the case of minimum transmitted energy $n=5,\ a=2$.

6. Conclusions

In the present contribution the hydroeastic response of a floating elastic breakwater in shallow water conditions is studied in terms of the characteristics of the reflected and transmitted waves. After a brief presentation of the governing equations, the equivalent variational problem is presented and a higher order finite element scheme is proposed for the calculation of the breakwater response. Next, the case

of a breakwater of constant stiffness has been considered, where a clear correlation between the employed Young's modulus and the amplitude and form of the transmitted pulse is shown. The transmitted wave energy was shown to be attenuated for increasing stiffness. In order to examine a case of variable elastic modulus a profile featuring periodic fluctuations was employed. In the employed profile, the Young's modulus is allowed to vary between a chosen set of minimum and maximum values while the number of periodic fluctuations and the steepness of the modulation peaks are controlled by parameters. Minimisation of the reflected energy was achieved when the wavelength of the periodic structure employed for the Young's modulus profile was comparable with the incoming wave excitation. A parametric study to further investigate the tuning of the employed stiffness profile parameters was carried out. Future developments involve incorporation of nonlinearities in the hydroelastic breakwater model.

References

[1] Stoker J J 1957 *Water Waves: the mathematical theory with applications* (New York: Interscience Publishers, Inc).
[2] Papathanasiou T K, Karperaki A E, Theotokoglou E E and Belibassakis K A 2015 Hydroelastic analysis of ice shelves under long wave excitation *Nat. Hazards Earth Syst. Sci.* **15** pp 1821-57.
[3] Squire V A 2008 Synergies between VLFS Hydroelasticity and Sea Ice Reasearch *Int. J. offshore polar* **18** pp 1-13.
[4] Wang C M and Tay Z Y 2015 Very Large Floating Structures: Applications, Research and Development *Proc Engineering* **14** pp 62-72.
[5] Wang C M, Watanabe E and Utsunomiya T 2008 *Very large floating structures*, (London: Taylor and Francis).
[6] Koutandos E, Prinos P and Gironella X 2005 Floating breakwaters under regular and irregular wave forcing: reflection and transmission characteristics *J. Hydraul. Res.* **43** pp 174-188.
[7] Meylan M H and Squire V A 1994 The response of ice floes to ocean waves *J. Geophys Res* **99** pp 891-900.
[8] Montiel F, Bennetts L G and Squire V A 2012 The transient response of floating elastic plates to wavemaker forcing in two dimensions *J. Fluids Struct.* **28** pp 416-433.
[9] Bennetts L G, Biggs N R T and Porter D A 2007 A multi-mode approximation to wave scattering by ice sheets of varying thickness *J. Fluid Mech.* **579** pp 413-43.
[10] Smith M J A and Meylan M H 2011 Wave scattering by an ice floe of variable thickness, *Cold Reg. Sci. Technol.* **67** pp 24-30.
[11] Sturova I V 2009 Time-dependent response of a heterogeneous elastic plate floating on shallow water of variable depth *J. Fluid Mech.* **637** pp 305-25.
[12] Praveen K M, Karmakar D, and Nasar T 2016 Hydroelastic analysis of floating elastic thick plate in shallow water depth *Perspect. in Sci.* **8** pp 770-72.
[13] Papathanasiou T K, Karperaki A, Theotokoglou E E and Belibassakis K A 2015 A higher order FEM for time-domain hydroelastic analysis of large floating bodies in an inhomogeneous shallow water environment *Proc. R. Soc. A* **471** 20140643.
[14] Papathanasiou T K and Karperaki A E 2017 Transmission and reflection of long waves over steep bathymetry variations using large floating strips of shallow draft *Proc of 7th Int. Conf.* on Computational Methods for Coupled Problems in Science and Engineering, COUPLED 2017 (12-14 June, Rhodes).
[15] Karperaki A E, Belibassakis K A and Papathanasiou T K 2016 Time-domain, shallow-water hydroelastic analysis of VLFS elastically connected to the seabed *Mar. Struct.* **48** pp 33-51.